CONTENTS

1. Structural Characterization Information

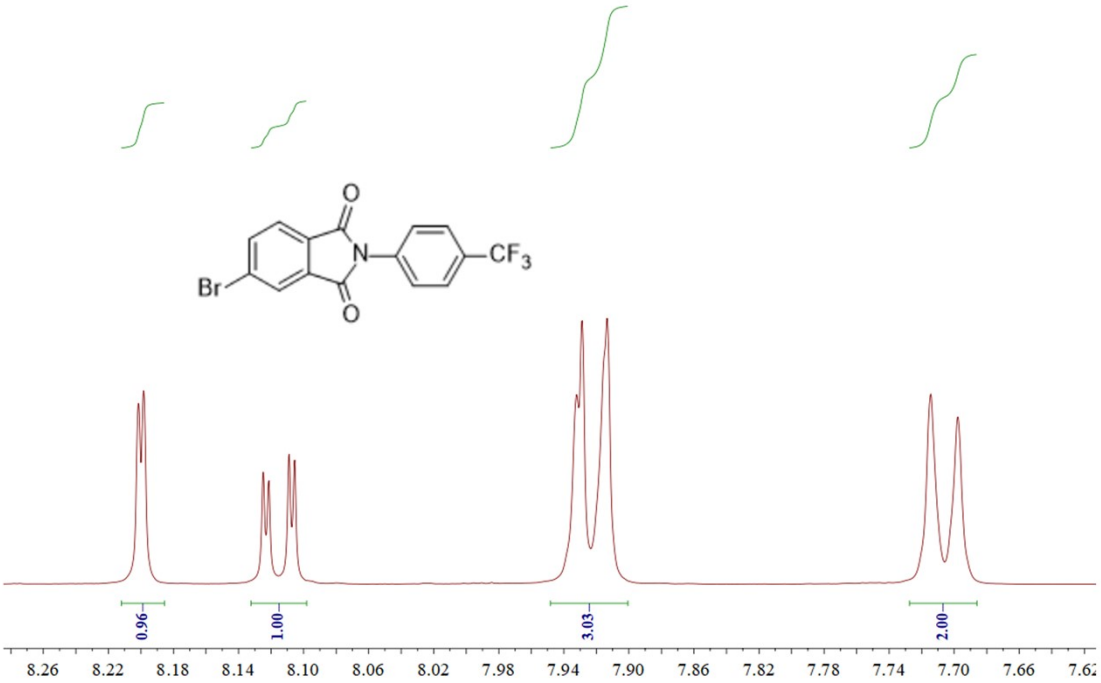

Figure S1. The ^{1}H NMR spectrum of 3FmBr in DMSO-d_6.

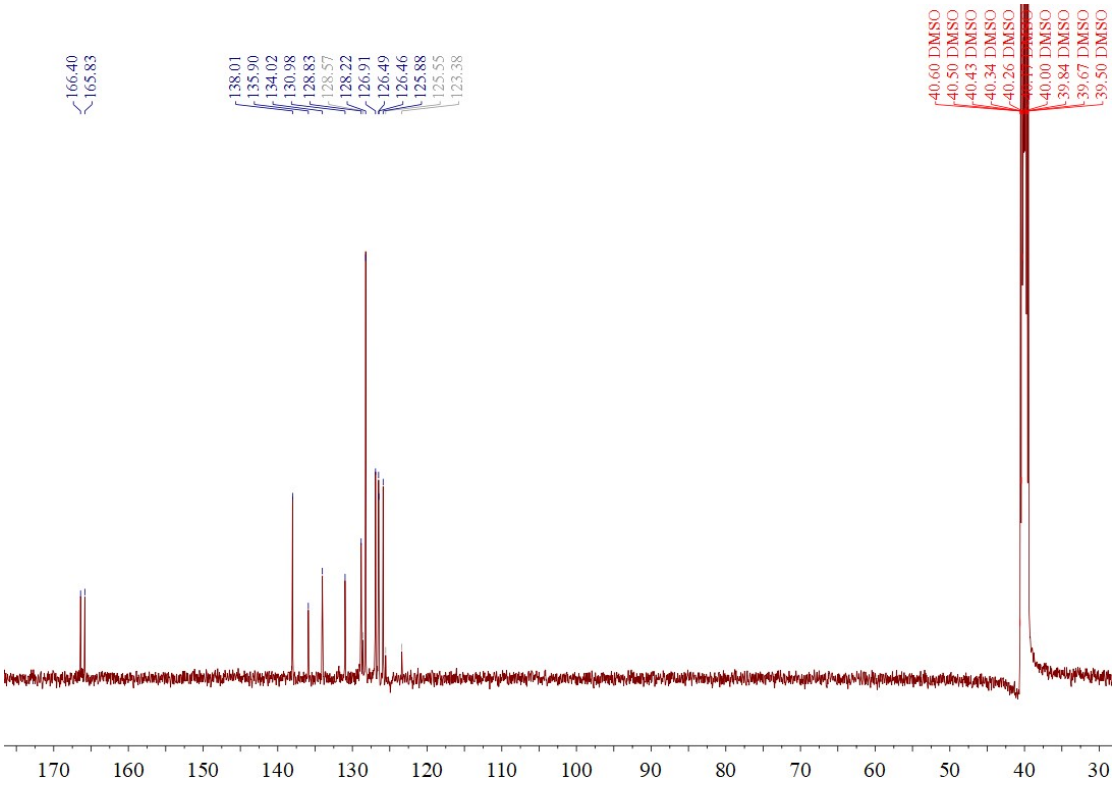

Figure S2. The ^{13}C NMR spectrum of 3FmBr in DMSO-d_6.

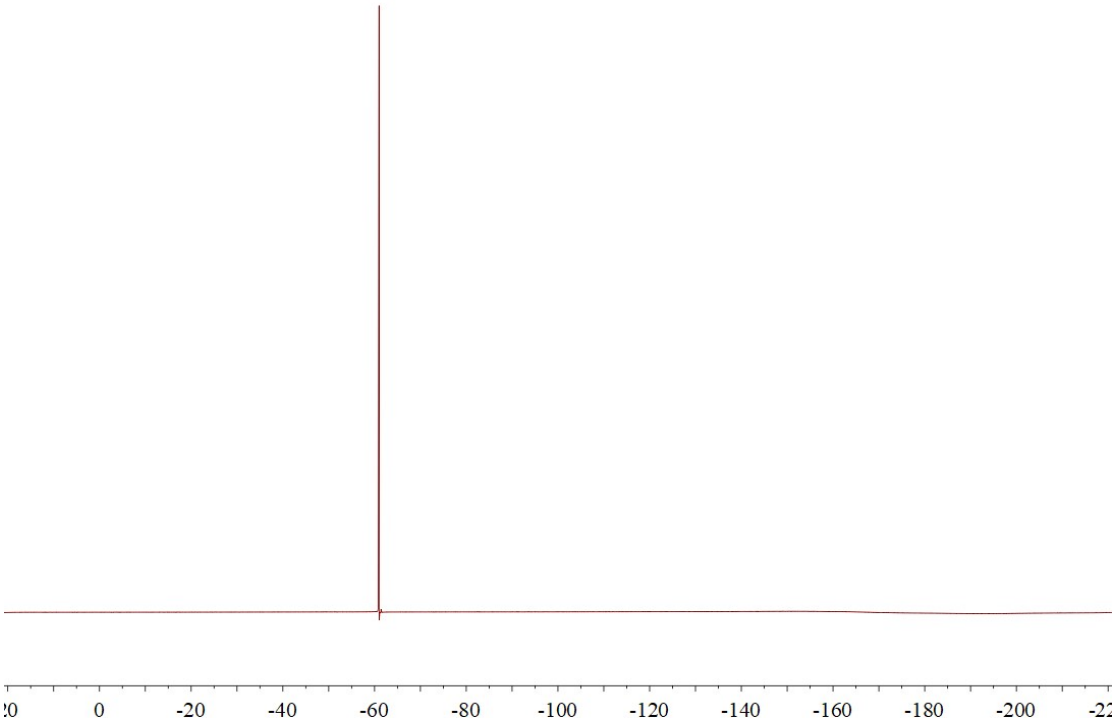

Figure S3. The ^{19}F NMR spectrum of 3FmBr in DMSO-d_6.

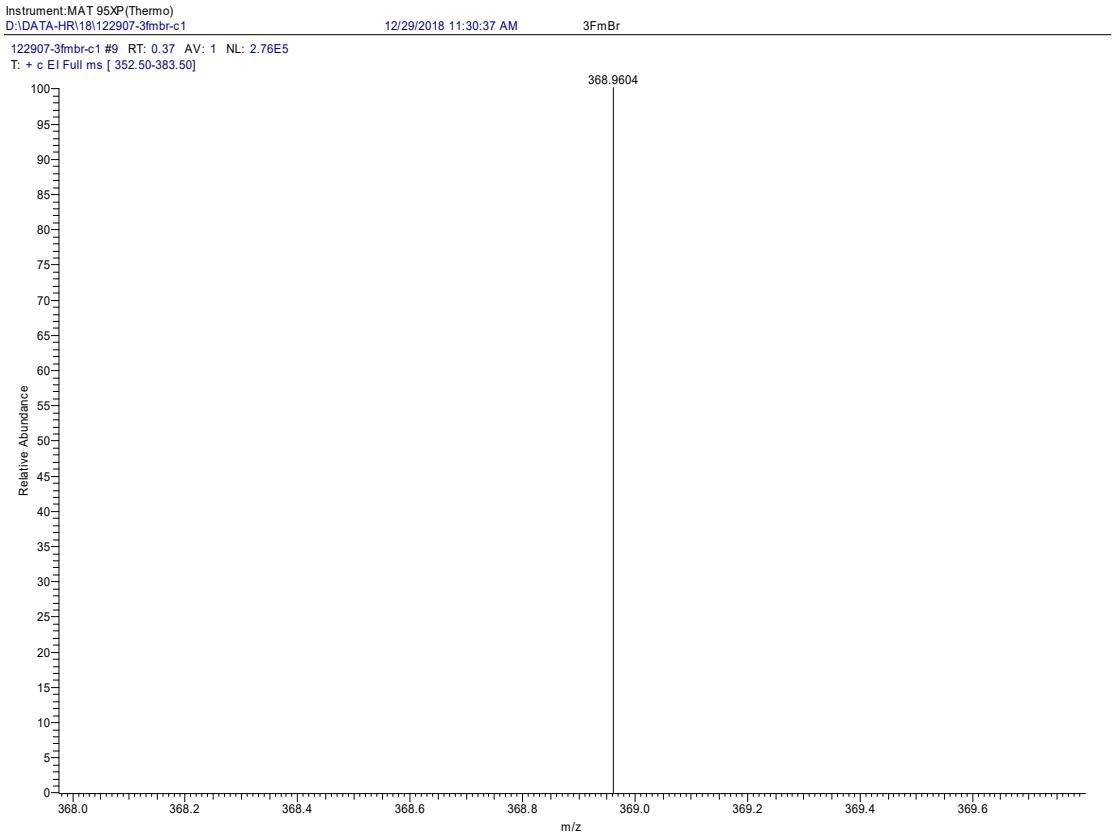

Figure S4. The high resolution mass spectra of 3FmBr.

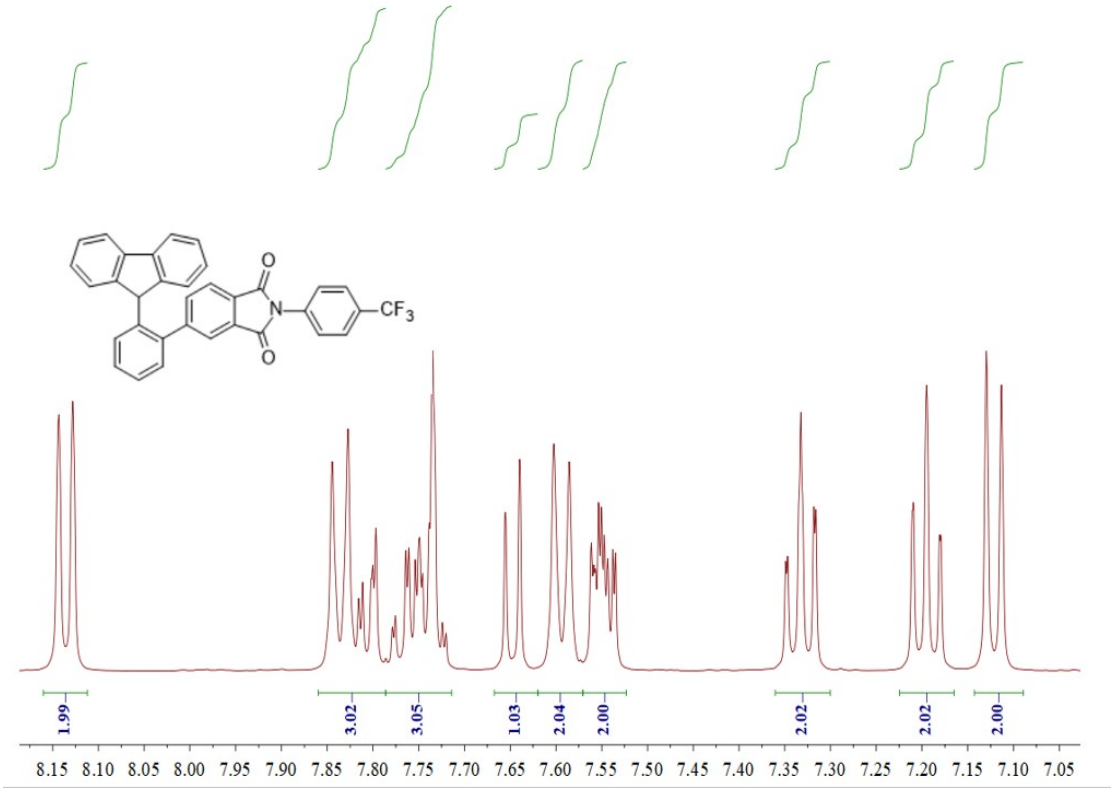

Figure S5. The ^{1}H NMR spectrum of 3Fmo in DMSO-d_6.

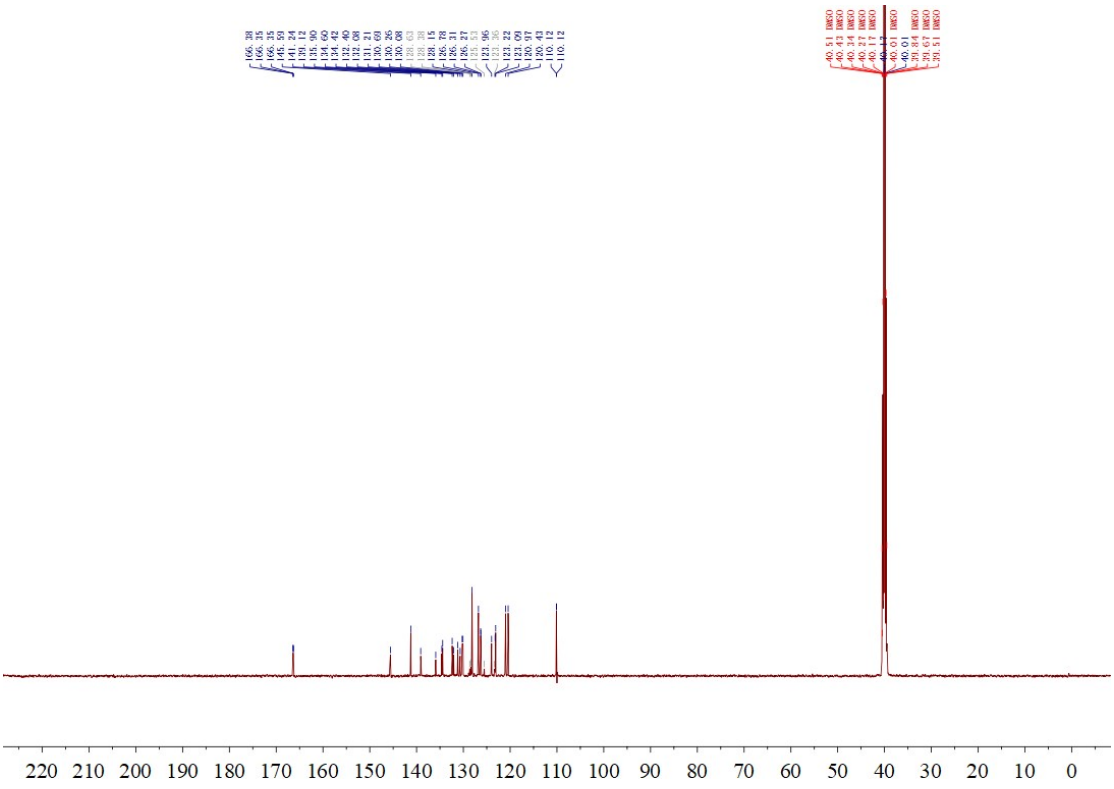

Figure S6. The ^{13}C NMR spectrum of 3Fmo in DMSO-d_6.

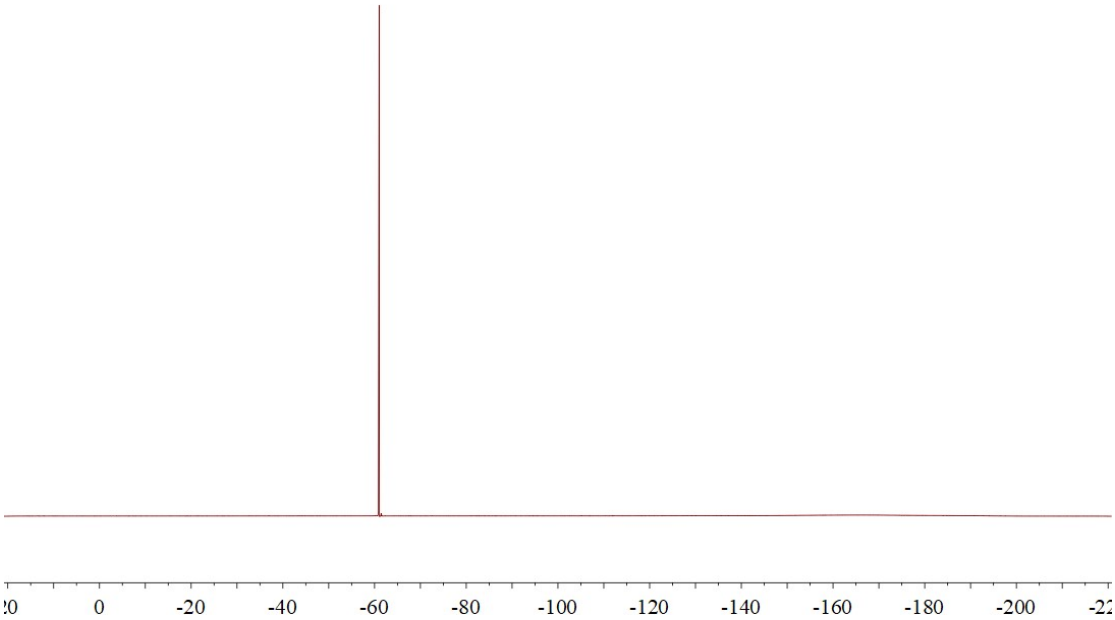

Figure S7. The ^{19}F NMR spectrum of 3Fmo in DMSO-d_6.

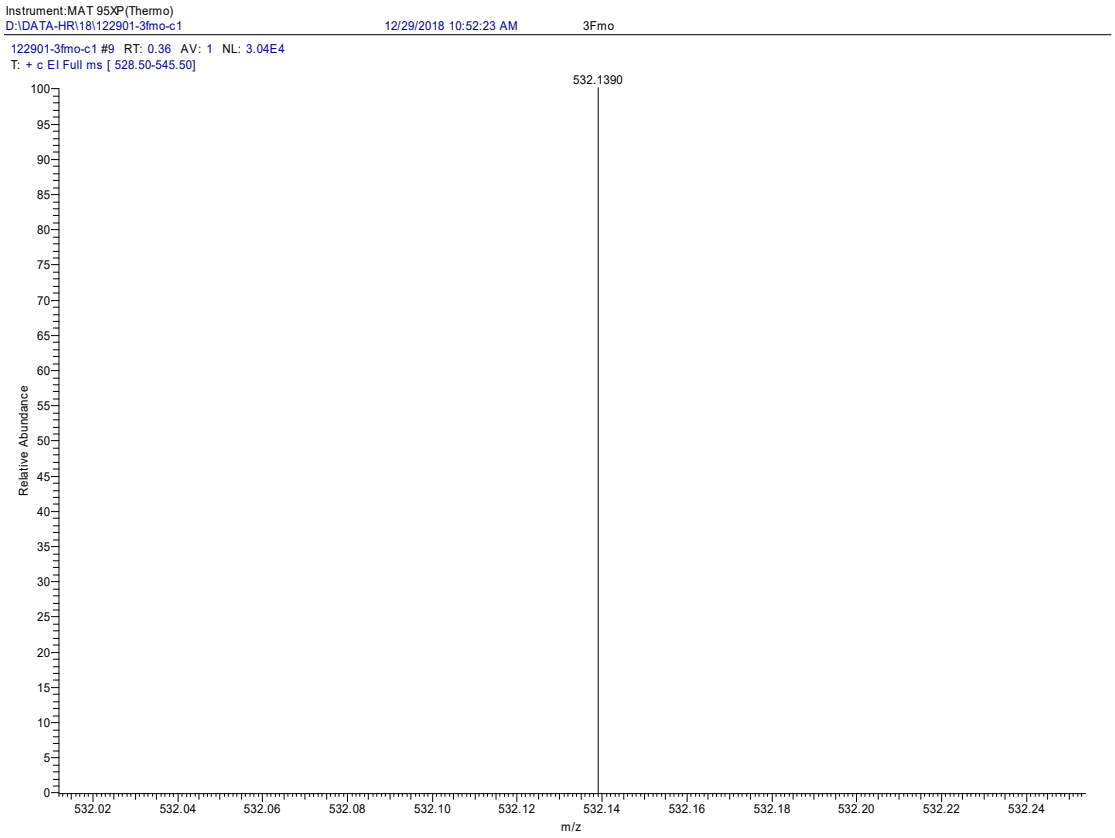

Figure S8. The high resolution mass spectra of 3Fmo.

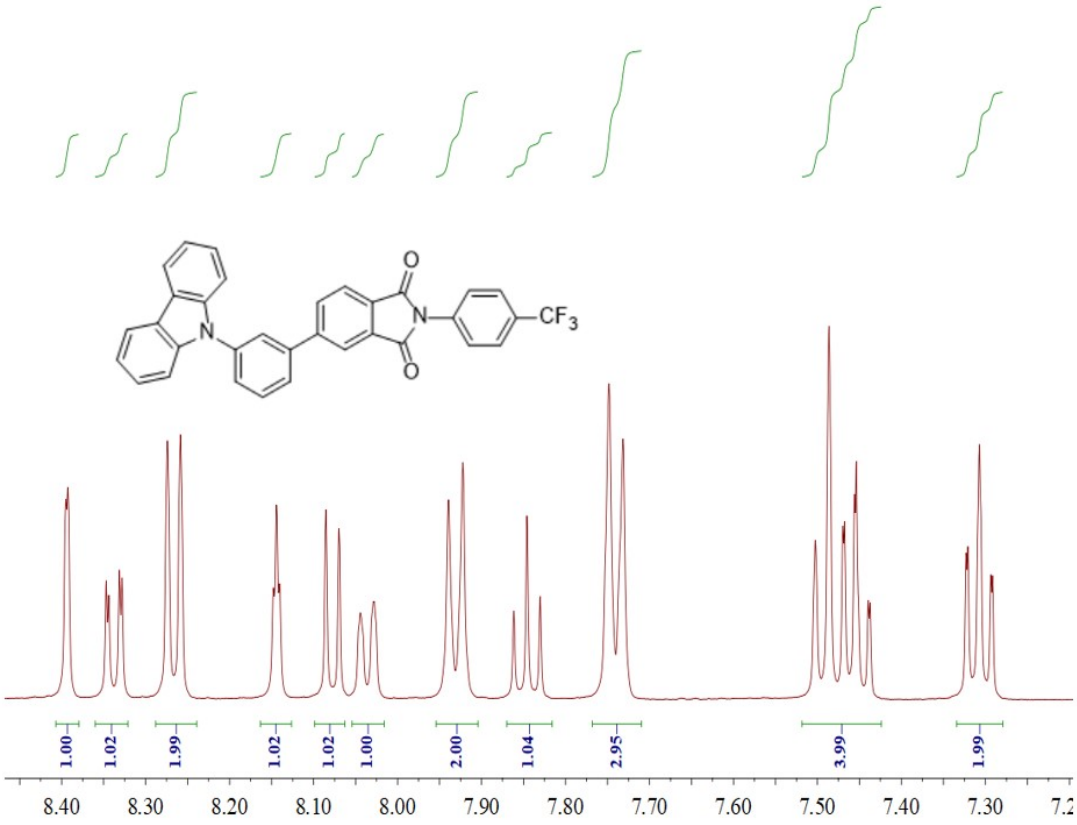

Figure S9. The ^{1}H NMR spectrum of 3Fmm in DMSO-d_6.

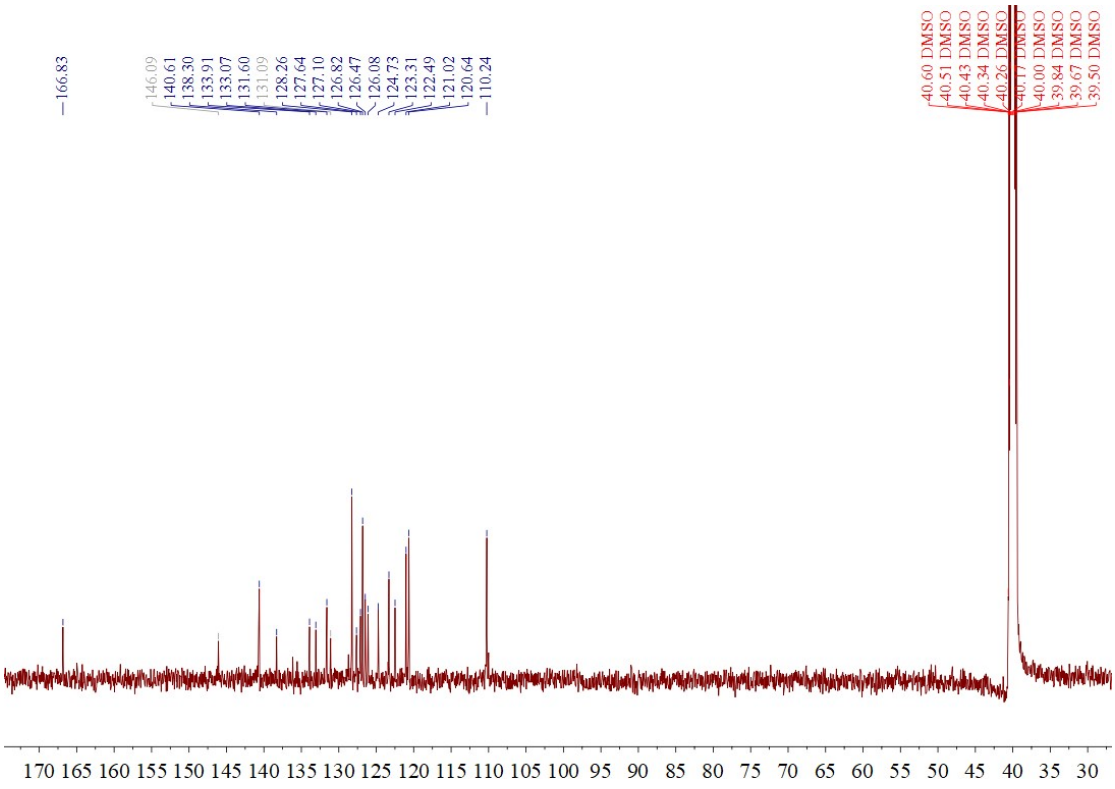

Figure S10. The ^{13}C NMR spectrum of 3Fmm in DMSO-d_6.

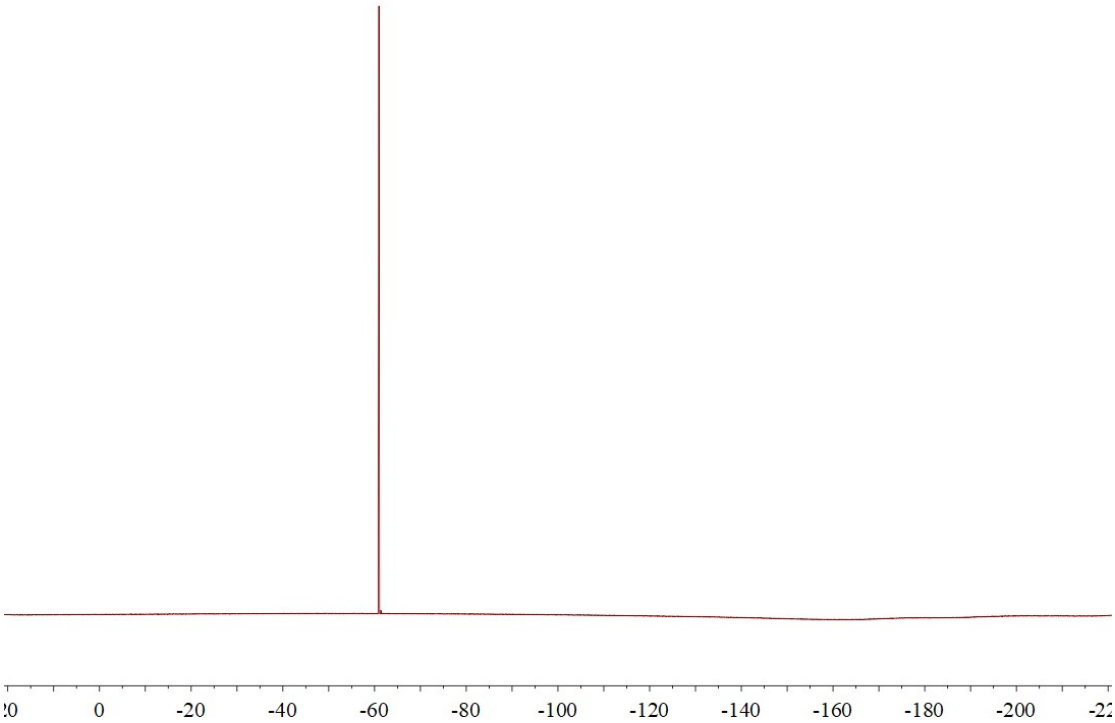

Figure S11. The ^{19}F NMR spectrum of 3Fmm in DMSO-d_6.

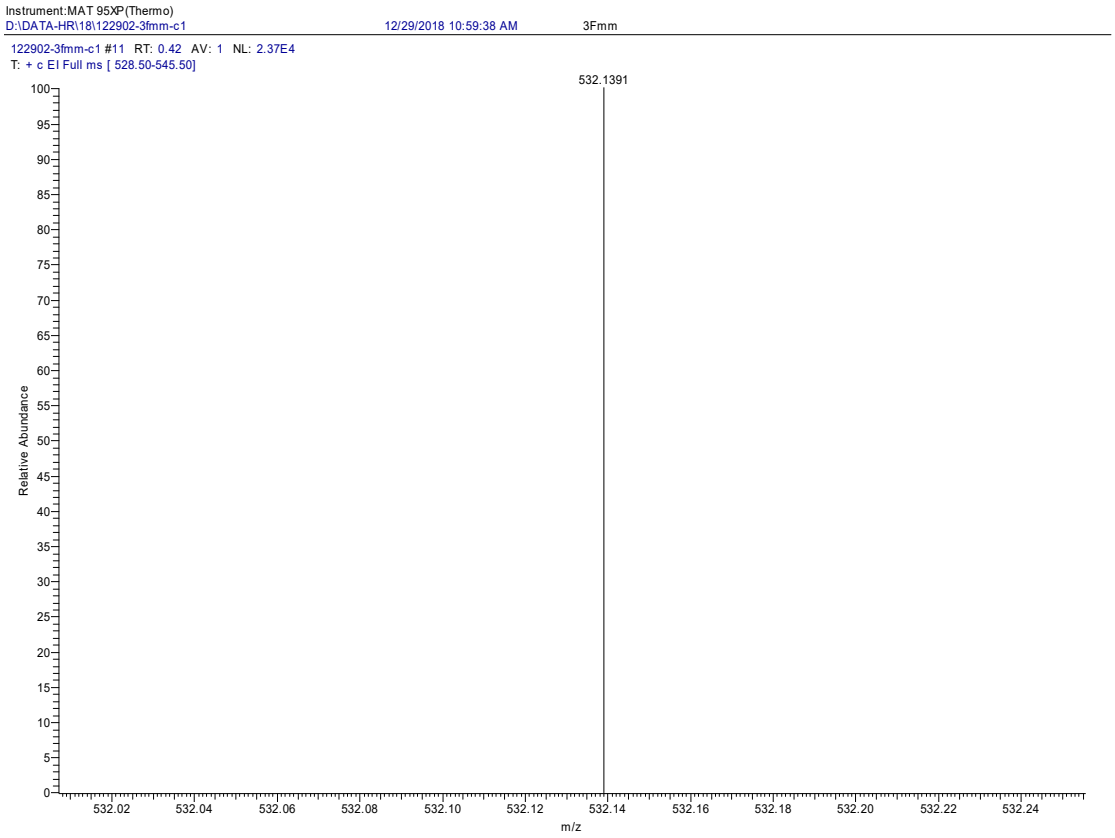

Figure S12. The high resolution mass spectra of 3Fmm.

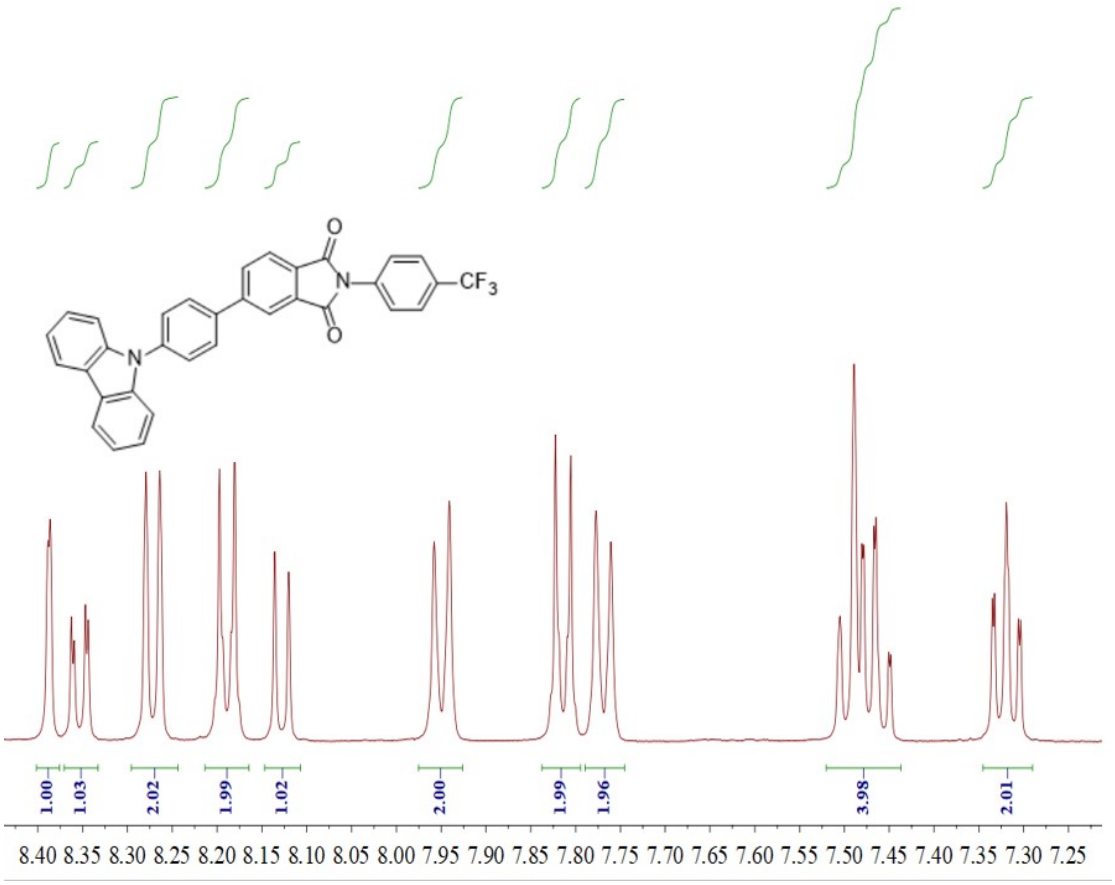

Figure S13. The ^{1}H NMR spectrum of 3Fmp in DMSO-d_6.

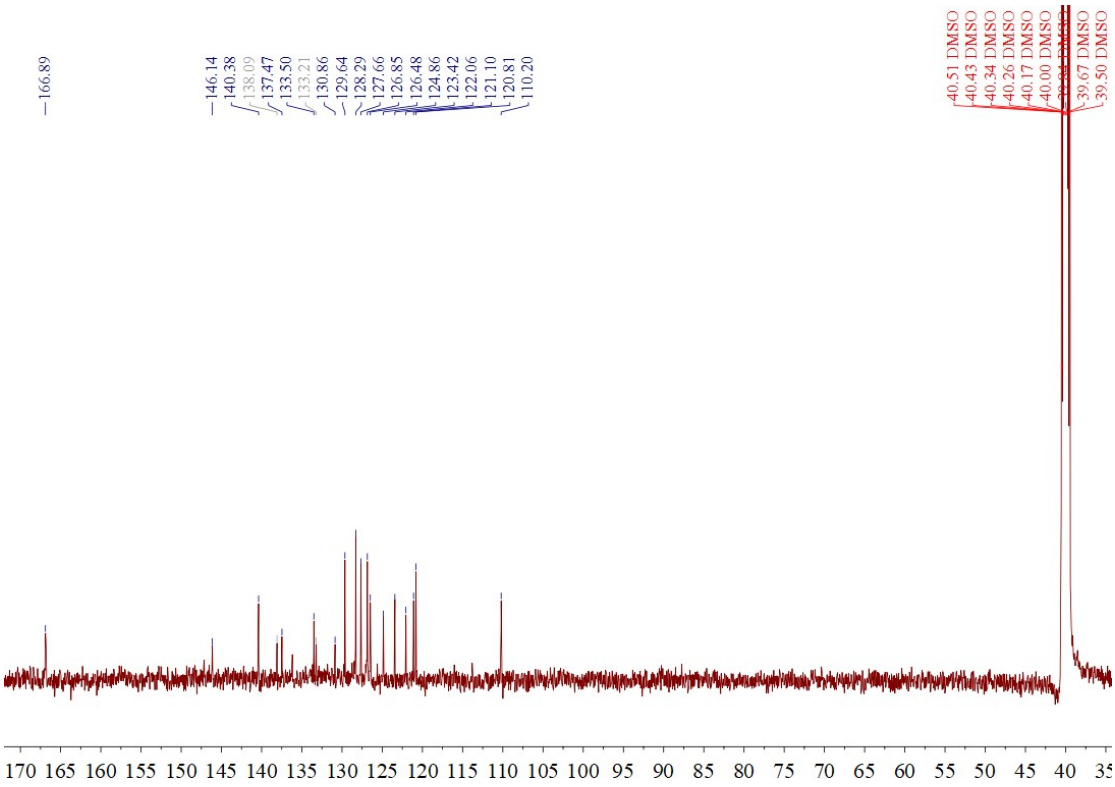

Figure S14. The ^{13}C NMR spectrum of 3Fmp in DMSO-d_6.

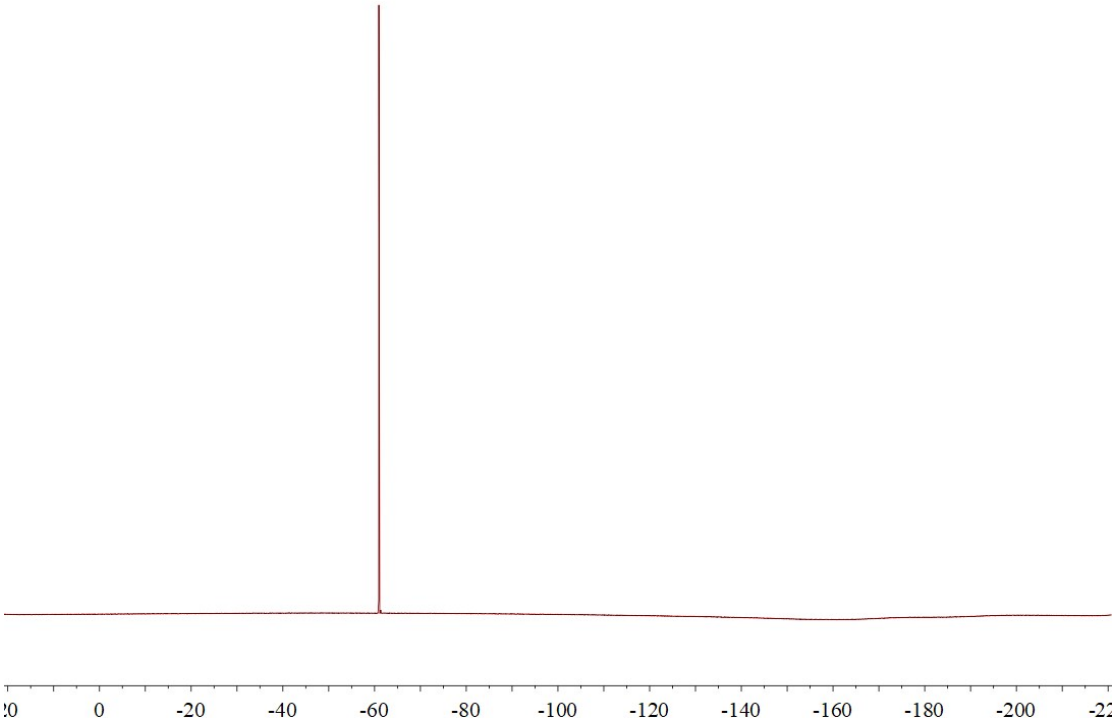

Figure S15. The ^{19}F NMR spectrum of 3Fmp in DMSO-d_6.

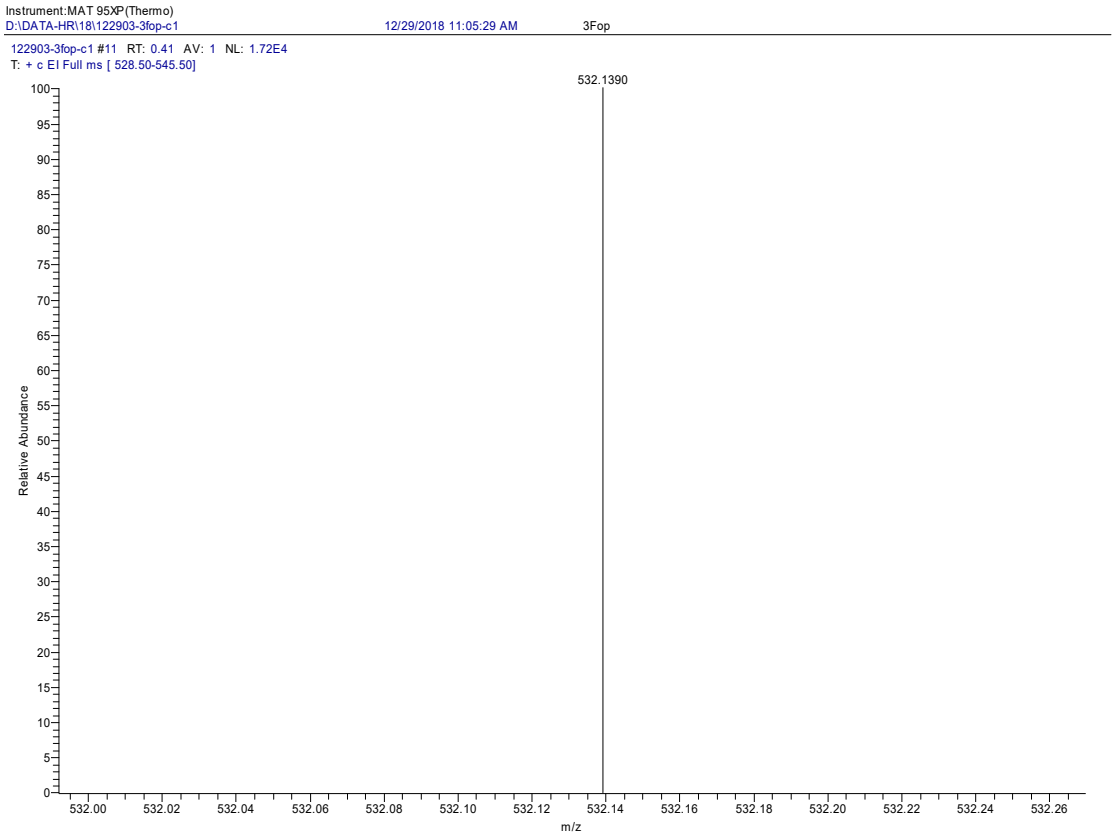

Figure S16. The high resolution mass spectra of 3Fmps.

2. Supporting Figures

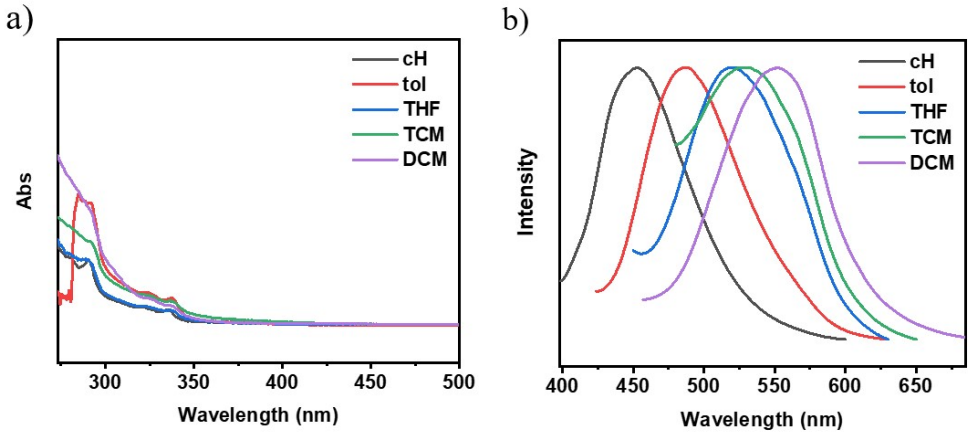

Figure S17. The UV-visible absorption spectrum (a) and fluorescence spectrum (b) of 3Fmo in dilute solutions (c=10^{-5} M) of varying polarity.

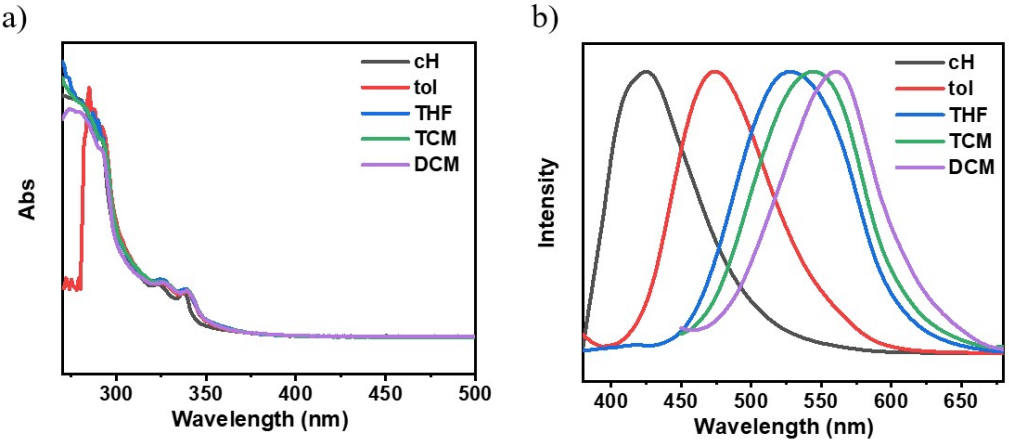

Figure S18. The UV-visible absorption spectrum (a) and fluorescence spectrum (b) of 3Fmm in dilute solutions (c=10^{-5} M) of varying polarity.

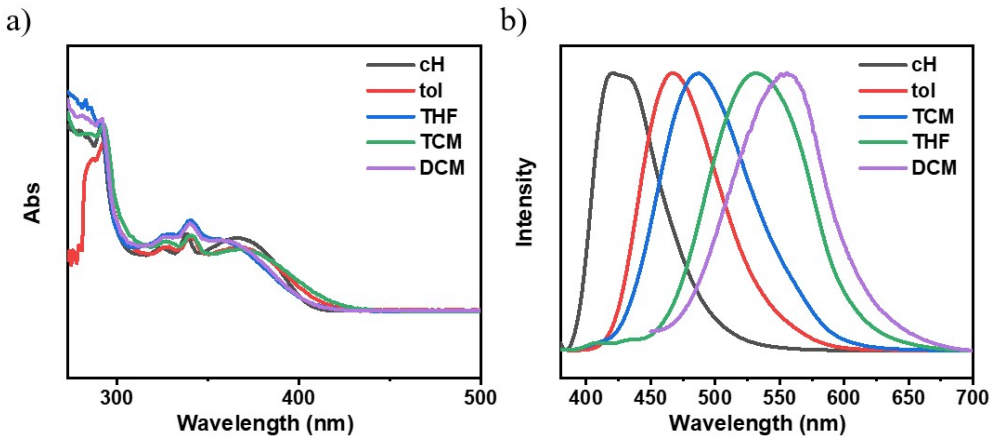

Figure S19. The UV-visible absorption spectrum (a) and fluorescence spectrum (b) of 3Fmp in dilute solutions (c=10^{-5} M) of varying polarity.

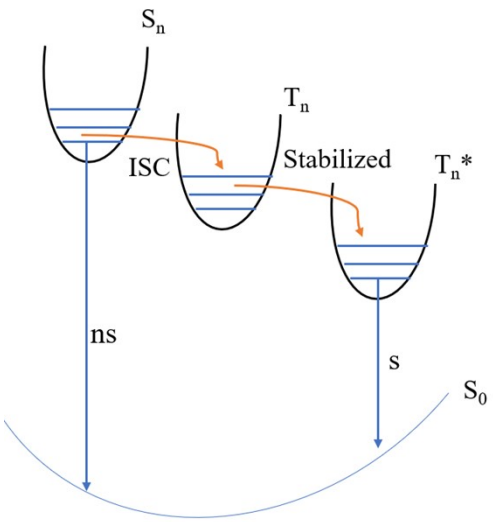

Figure S20. Schematic diagram of the multi-molecular phosphorescence emission process.

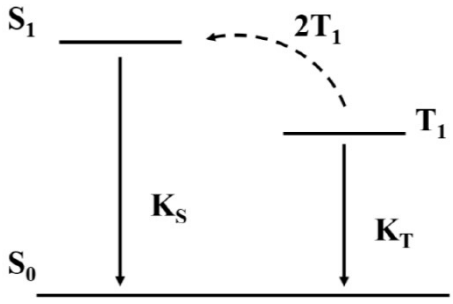

Figure S21. Schematic diagram of the TTA emission mechanism.

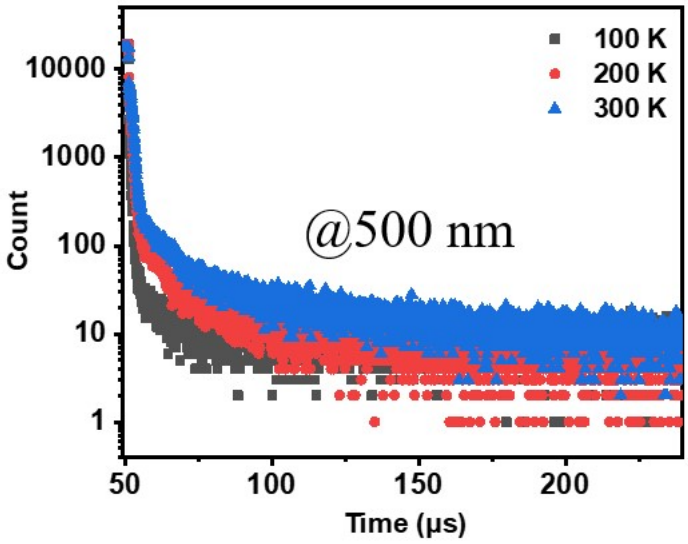

Figure S22. Temperature-dependent lifetimes of the excited state associated with the 500 nm emission peak in 3Fmo powder.

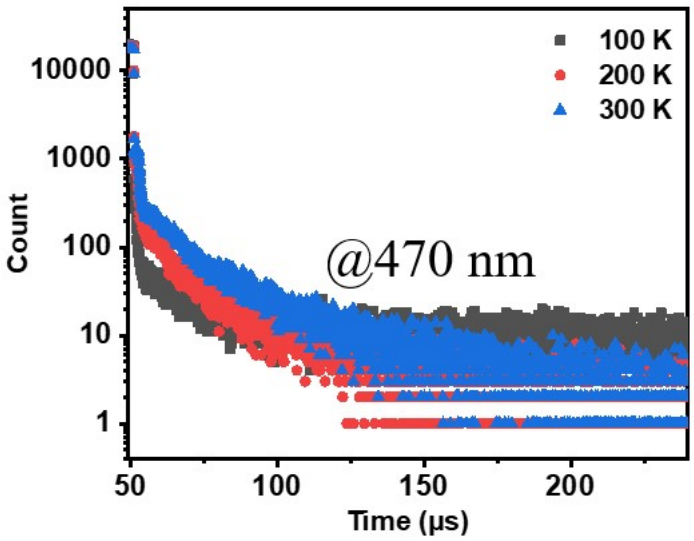

Figure S23. Temperature-dependent lifetimes of the excited state associated with the 470 nm emission peak in 3Fmp powder.

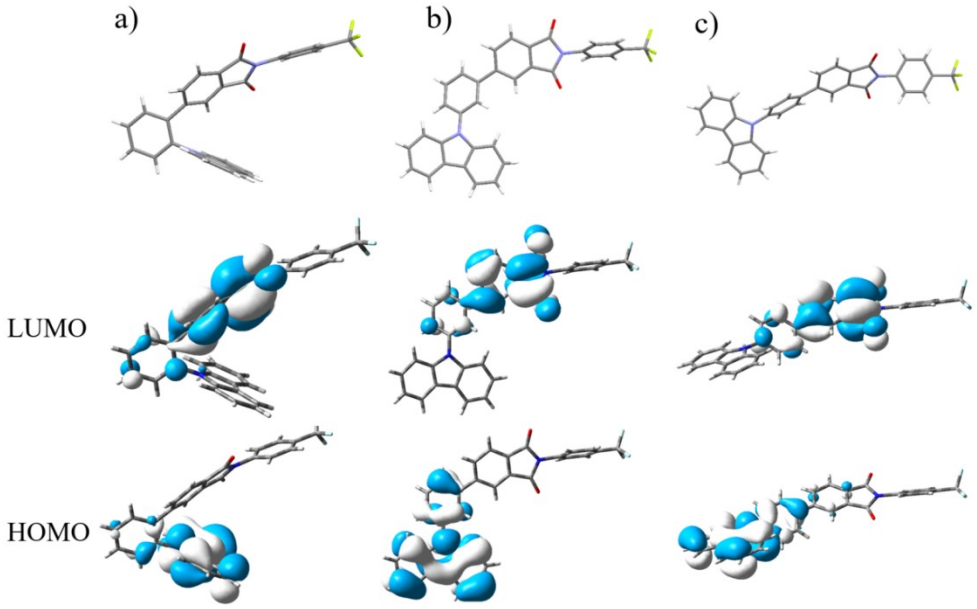

Figure S24. The single-crystal structures and distributions of electron density for the compounds are identified as: a) 3Fmo; b) 3Fmm; c) 3Fmp.

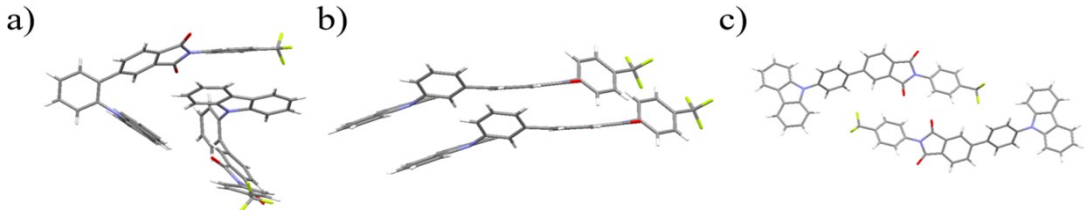

Figure S25. Interaction of molecules in the crystal: a) 3Fmo; b) 3Fmm; c) 3Fmp.

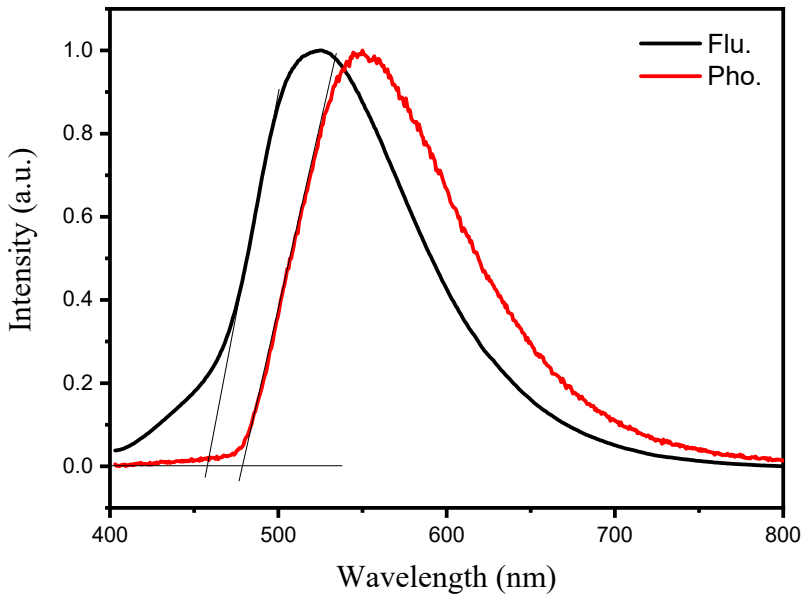

Figure S26. The fluorescence and phosphorescence spectra of 3Fmo.

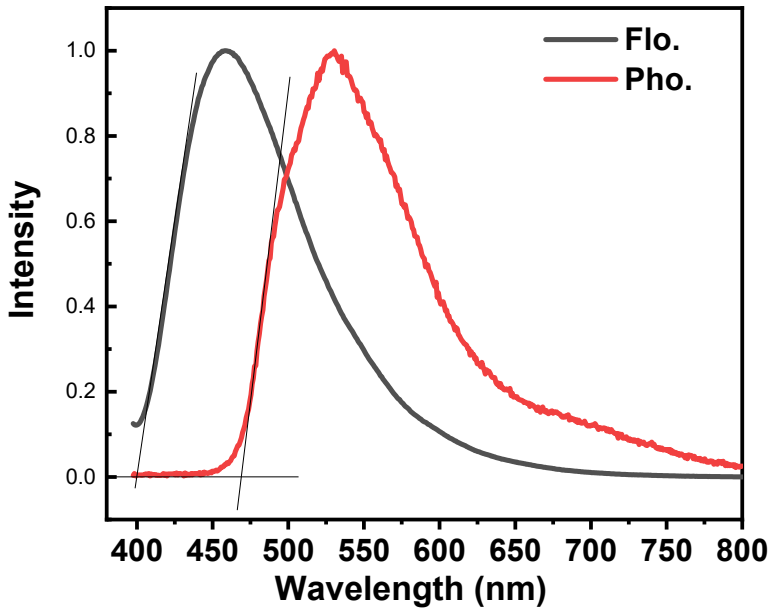

Figure S27. The fluorescence and phosphorescence spectra of 3Fmm.

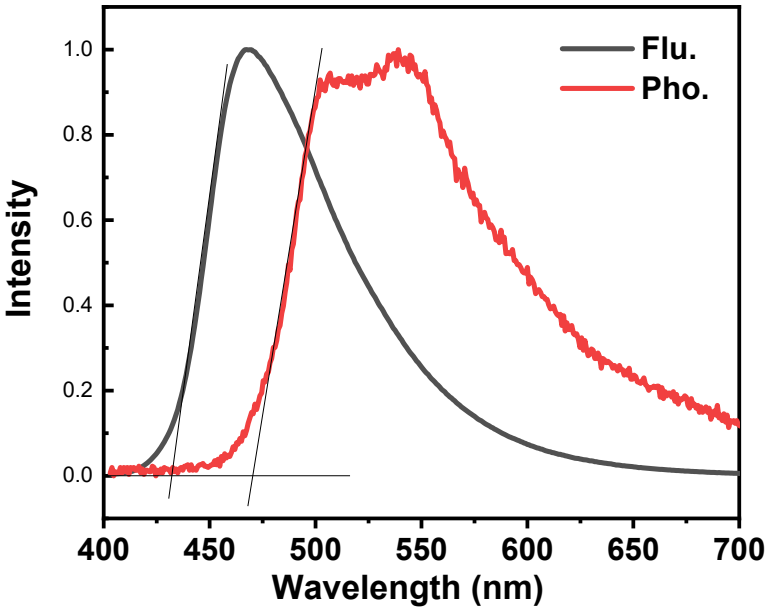

Figure S28. The fluorescence and phosphorescence spectra of 3Fmp.

3. Supporting Tables

Table S1. Photophysical properties of the compound powder

	3Fmo	3Fmm	3Fmp
$\lambda_{max}^{em}\ (nm)$	494	456	468
λ_{max}^{abs} **(nm)**	429	378	421
λ_{max}^{ex} **(nm)**	486	385	454
τ (μs)	2.25	59.6	11.7

Table S2. Crystal data and structure refinement for 3Fmo

Identification code	**3Fmo**
Empirical formula	$C_{33}H_{19}F_3N_2O_2$
Formula weight	532.50
Temperature/K	292.9(3)
Crystal system	monoclinic
Space group	$P2_1/n$
a/Å	14.1951(3)
b/Å	10.5832(2)
c/Å	17.5467(3)
α/°	90
β/°	98.318(2)
γ/°	90
Volume/Å^3	2608.30(9)
Z	4
ρ_{calc}g/cm^3	1.356
μ/mm^{-1}	0.832
F(000)	1096.0
Crystal size/mm^3	0.400 × 0.300 × 0.060
Radiation	CuKα (λ = 1.54184)
2Θ range for data collection/°	7.502 to 149.844
Index ranges	$-14 \le h \le 17$, $-12 \le k \le 8$, $-19 \le l \le 21$
Reflections collected	8076
Independent reflections	5132 [R_{int} = 0.0251, R_{sigma} = 0.0339]
Data/restraints/parameters	5132/0/361
Goodness-of-fit on F^2	1.048
Final R indexes [I>=2σ (I)]	R_1 = 0.0643, wR_2 = 0.1798

Final R indexes [all data]	R_1 = 0.0772, wR_2 = 0.1967
Largest diff. peak/hole / e Å-3	0.58/-0.42

Table S3. Crystal data and structure refinement for 3Fmm.

Identification code	**3Fmm**
Empirical formula	$C_{33}H_{19}F_3N_2O_2$
Formula weight	532.50
Temperature/K	150.00(10)
Crystal system	monoclinic
Space group	$P2_1/c$
a/Å	26.4492(10)
b/Å	16.7231(6)
c/Å	5.3699(2)
α/°	90
β/°	94.146(4)
γ/°	90
Volume/Å^3	2368.96(15)
Z	4
ρ_{calc}g/cm^3	1.493
μ/mm^{-1}	0.916
F(000)	1096.0
Crystal size/mm^3	? × ? × ?
Radiation	CuKα (λ = 1.54184)
2Θ range for data collection/°	17.386 to 148.082
Index ranges	$-32 \leq h \leq 27$, $-17 \leq k \leq 20$, $-4 \leq l \leq 6$
Reflections collected	7230
Independent reflections	3890 [R_{int} = 0.0801, R_{sigma} = 0.0622]
Data/restraints/parameters	3890/0/361
Goodness-of-fit on F^2	1.070
Final R indexes [I>=2σ (I)]	R_1 = 0.0901, wR_2 = 0.2456
Final R indexes [all data]	R_1 = 0.1138, wR_2 = 0.2670
Largest diff. peak/hole / e Å^{-3}	0.40/-0.40

Table S4. Crystal data and structure refinement for 3Fmp.

Identification code	**3Fmp**
Empirical formula	$C_{33}H_{19}F_3N_2O_2$
Formula weight	532.50
Temperature/K	150.00(10)
Crystal system	monoclinic
Space group	$P2_1/c$

a/Å	9.9603(2)
b/Å	7.8995(2)
c/Å	32.1373(6)
α/°	90
β/°	93.108(2)
γ/°	90
Volume/Å^3	2524.89(9)
Z	4
ρ_{calc}g/cm^3	1.401
μ/mm^{-1}	0.860
F(000)	1096.0
Crystal size/mm^3	1.800 × 0.090 × 0.050
Radiation	CuKα (λ = 1.54184)
2Θ range for data collection/°	8.892 to 134.224
Index ranges	-11 ≤ h ≤ 11, -6 ≤ k ≤ 9, -37 ≤ l ≤ 33
Reflections collected	7581
Independent reflections	4312 [R_{int} = 0.0396, R_{sigma} = 0.0406]
Data/restraints/parameters	4312/0/361
Goodness-of-fit on F^2	1.046
Final R indexes [I>=2σ (I)]	R_1 = 0.0418, wR_2 = 0.1035
Final R indexes [all data]	R_1 = 0.0499, wR_2 = 0.1099

Table S5. Translation of electronic energy levels obtained from the single-crystal studies of three compounds.

Structure	**HOMO (eV)**	**LUMO (eV)**	**ΔE_g (eV)**	**Dipole**	**T_1 (eV)**	**S_1 (eV)**	**ΔE_{ST} (eV)**
3Fmo	-5.85	-2.76	3.09	7.77	2.54	2.57	0.03
3Fmm	-5.81	-2.65	3.16	5.93	2.70	2.78	0.08
3Fmp	-5.84	-2.92	2.92	6.07	2.41	2.59	0.18